INTERNATIONAL JOURNAL OF INTEGRATED ENGINEERING
ISSN: 2229-838X e-ISSN: 2600-7916

IJIE

Vol. 17 No. 6 (2025) 147-158
https://publisher.uthm.edu.my/ojs/index.php/ijie

Gain Enhanced On-chip Monopole Antenna Utilizing Dual Rectangular Patch Artificial Magnetic Conductor at 5.8 GHz

Bello Muhammad Abdullahi[1,3], Mohd Fadzil Ain[1]*, Ahmadu Girgiri[1,4], Mohd Nazri Mahmud[1], Mohd Zamir Pakhuruddin[2]

[1] *School of Electrical and Electronic Engineering, Universiti Sains Malaysia, Engineering Campus, 14300, Nibong Tebal, MALAYSIA*
[2] *School of Physics, Universiti Sains Malaysia, Main Campus 11800, Penang, MALAYSIA*
[3] *Abdu Gusau Polytechnic, 1021, Talata Mafara, Zamfara, NIGERIA*
[4] *Mai Idris Alooma Polytechnic, 1020, Geidam, Yobe, NIGERIA*

*Corresponding Author: eemfadzil@usm.my
DOI: https://doi.org/10.30880/ijie.2025.17.06.012

Article Info

Received: 20 March 2025
Accepted: 28 October 2025
Available online: 30 December 2025

Keywords

On-chip antenna, dual rectangular patch, artificial magnetic conductor, gain, radiation efficiency, reflection phase

Abstract

The rising popularity of chip-based wireless devices has incited greater attention in on-chip antenna (OCA) technology due to its compact size, low power consumption, and ease of integration into footprint chip-size transceivers. However, OCAs face challenges such as low gain, poor radiation efficiency, and a distorted radiation pattern due to the inherited low resistivity, and high permittivity lossy silicon substrate. This study introduces the dual-rectangular patch (DRP) structured artificial magnetic conductor (AMC) for the enhancing the performance of OCA. Thus, investigates the effect of the gain, and radiation efficiency of the proposed design. A DRP-AMC was developed as a modified AMC reflective surface, optimized to boost the gain and characteristic of the antenna at 5.8 GHz. To assess the design performance, the antenna prototype is fabricated and measured. As a result, an increase gain of 40.2% compared to the non-AMC-inspired model and 29.2% over the single-rectangular patch (SRP) model. This improvement is attributed to the DRP-AMC's performance, making this antenna suitable for Wi-fi 6, RFID, and WiMAX applications at 5.8 GHz.

1. Introduction

Over the past few years, there have been notable progressions in developing chip-based wireless systems. These improvements have been driven by the need for novel applications that demand high data rates, cost-effectiveness, compact size, and material stability antennas [1]. As a result, an On-chip antenna (OCA) is considered a potential alternative due to its inherent benefits, including its small size and low energy consumption [2], [3]. It is a contemporary antenna technology that enables the integration of radio frequency (RF) circuitry on the same silicon chip [4]. Thus, offers seamless integration with the capacity to facilitate high-speed wireless communication [5]. It supports a wide range of application in the lower and high-frequency based wireless devices, such as wireless transceivers, wireless fidelity, and Internet-of-Things based on users' demand due to their low profile and compact chip-size [6]. For instance, IoTs are anticipated to be the next advancing wireless technology, providing societal connectivity, according to Transform Insights TAM. There were approximately 7.6 billion active IoT devices in late 2019, projected to exceed 24 billion by 2030[7], in which OCAs are at the fore front potential antennas.

OCA enables integration into the radio circuit using a single-chip module (SCM) or a multi-chip module (MCM) [1] based on the design and target application. Integrating OCA requires a small chip with minimal space requirements. It is commonly set up in a multi-layer structure consisting of metal, insulator, and semiconductor materials [8]. Despite its benefits, it suffers from low gain, diminished radiation efficiency, and distorted radiation patterns [9],[10]. These challenges mainly stem from the inherent properties of silicon, which include low resistivity and high permittivity. These issues have incited extensive efforts to achieve optimal gain and efficient radiation characteristic on-chip antenna using a modified performance improvement technique. Prior research has proposed various OCA performance strategies tailored to specific applications and frequency ranges. Potential methods include artificial magnetic conductor (AMC) [11], dielectric resonator loading (DRL), super-substrate loading, micromachining [12], substrate thinning, and ion implantation [8], [13]. However, further research on performance improvements, particularly the efficiency, radiation resistance, and the working gain have become significant. The AMC approach is widely favored due to its excellent reflection properties, low production cost, and it requires minimal metal film.

An AMC is a synthetically created periodic structure characterized by a high-impedance surface with zero-reflection phase properties [13], [14]. The device prevents electromagnetic waves from penetrating the lossy silicon substrate by separating it from the incoming wave and acting as a reflector [9]. Integrating the AMC structure into the OCA stack-up layers is a promising approach for enhancing performance. In addition, AMC and metasurface based technology support integration into high frequency OCA design for large wireless terminals, as the combined technology shrink antenna size [15]. Numerous studies have highlighted the importance of AMC techniques in improving gain and radiation efficiency in OCA designs. For example, in [16], a meandered bowtie integrated OCA with a dual dipole patch AMC demonstrated improved gain, ranging from 4.15 to 4.93 dB, compared to a single-dipole AMC structure. Likewise, [11] proposed a square-loop structured AMC embedded into a six-layer stack-up OCA model, achieving an intrinsic gain of -1.4 dB, an 8 dB improvement over the non-AMC embedded OCA model. An H-shaped AMC model incorporated into an on-chip antenna (OCA) is presented in [12], resulting in a 19% efficiency improvement and a 0.77 dB increase in peak gain compared to non-AMC designs. Additionally, [17] utilizes a double-layer AMC to achieve enhancements, featuring a metal tiling-like configuration embedded within layers of SiO2 material. Various AMC models demonstrate different performances, necessitating adjustments to the AMC pattern to optimize OCA performance for specific applications. For instance, single-patch AMC and double-layer AMC each exhibit distinct performance characteristics.

This study reports a design of enhanced gain monopole planar on-chip antenna inspired by a modified AMC, dual rectangular patch (DRP) structure as in Fig. 1(b), and its characteristics were determined. Thus, a 4x4 array of the optimized AMC was incorporated into the chip. This inclusion substantially increased gain by 40.2 % and 29.2 % over the single rectangular patch (SRP)- AMC model design shown in Fig. 1(c) . This article is organized as follows: Section 2 outlines the suggested antenna model and configuration, DRP-AMC configuration, and its characteristic focusing on the principle of OCA multi-layered structure. It reports the simulation, measurement and the results validation in Section 3. Finally, Section 4, summarizes the study findings and the antenna performance.

2. Antenna Design and Configuration

This part discusses the OCA design, and the analysis of its model structure consisting of the layers of silicon (Si), silicon oxide (SiO2), and metallic plates arranged in a stacked configuration, as presented in Fig. 1(a). The model was designed and simulated using 3D EM CST studio. Following CMOS design principles, the antenna prototype was developed using magnetron sputtering and vapour deposition technologies. Initially, a 2 μm thick SiO_2 layer was deposited as the first insulation layer on a 500 μm bulk silicon substrate. This was followed by depositing a 1 μm thick DRP-AMC layer using silver electrically conductive epoxy. The second layer of SiO_2 layer deposited by repeating the initial process. A monopole structured radiating conductor (M1) was then deposited on the second SiO_2 layer as the stacked layer shown in Fig. 1(a). The SiO_2 offers insulation between the Si-substrate and M2, as well as M1 and M2 due to its outstanding insulation properties and electrical bandgap of approximately 8.9 eV [18]It has an estimated dielectric constant of 3.85, at the layer thickness of 2 μm for this design. Thus, operates within a high electrical resistivity of 10^{14} to 10^{16} Ω·cm. However, M2 is the periodic DRP-AMC layer that shields the migrating incidence from the top antenna into the lossy Si substrate with typically low resistivity (1-15 Ω-cm) of the bulk silicon chip [19]. Thus, prior to the proposed DRP-AMC incorporated design shown in Fig. 1 (a), the SRP-AMC inspired design in Fig. 2(C) was incorporated into the antenna chip and simulated. Hence, the performance of the antenna were recorded. . Table 1 provides the optimized parameters of the suggested antenna.

Int. Journal of Integrated Engineering Vol. 17 No. 6 (2025) p. 147-158

Table 1 *Optimized parameters of the proposed antenna*

Parameter	Value(mm)	Parameter	Value(mm)
Lx	4.5	Wa	6.0
Lr	8.92	d	0.73
Lp	15.5	fL	10.2
L1	9.4	S	1.0
Pw	0.75	y	1.8
hsi	0.50	tm	0.001
hs	0.002	g	0.3
Wp	11.5	PL	2.125

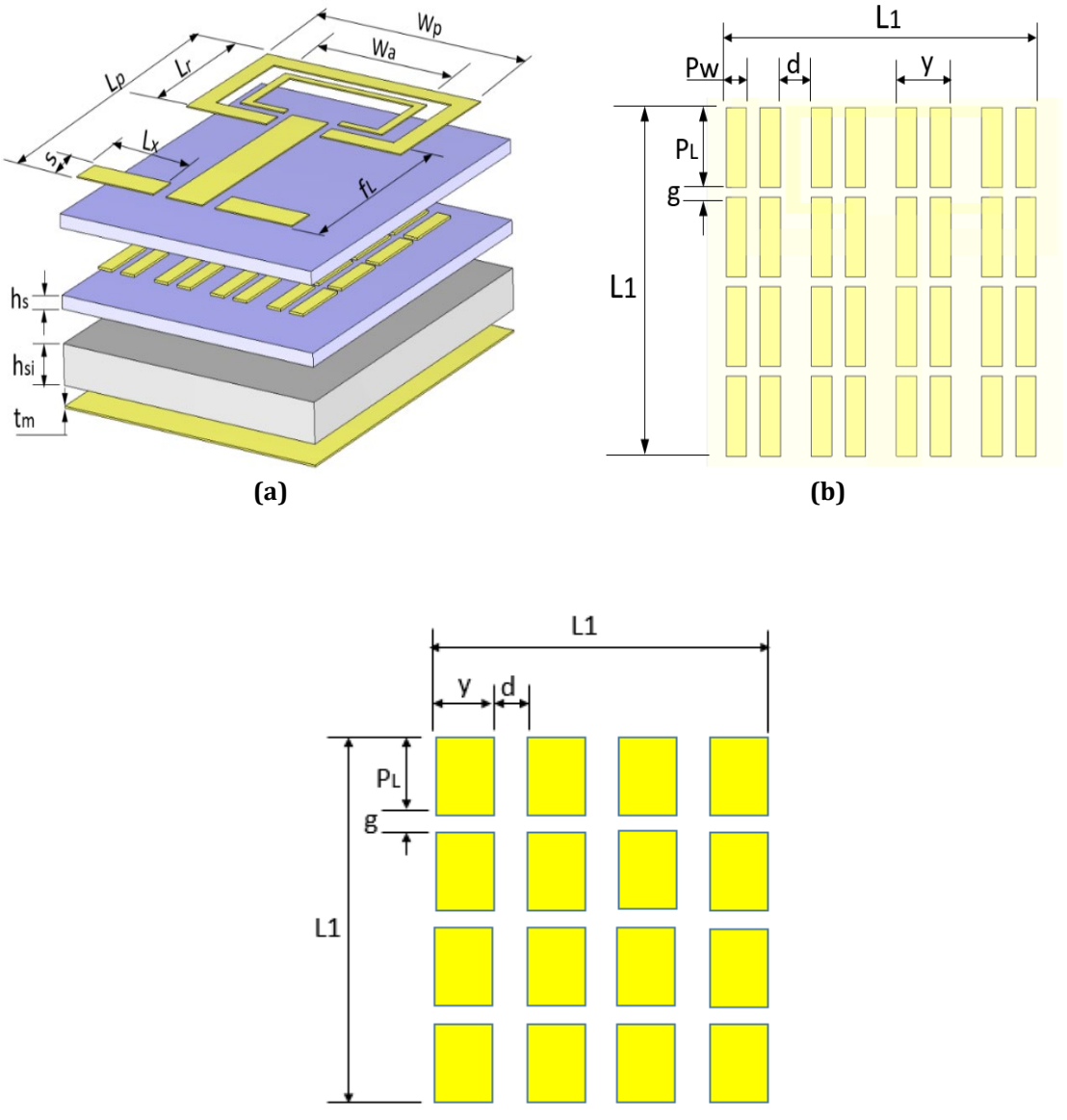

Fig. 1 *The proposed OCA structure (a) Stacked layer; (b) DRP-AMC model; (c) SRP-AMC model*

2.1 Design of SRP-AMC model

Prior to the design of the proposed dual rectangular patch (DRP) artificial magnetic conductor (AMC), a conventional single rectangular patch (SRP) AMC unit cell shown in Fig. 2(a) was first simulated using a periodic structure setup with defined boundary conditions and an excitation port. A frequency domain solver was employed to assess the performance of the structure by adjusting the unit cell until the desired zero-phase resonance and bounded within the reflection phase from -90° to +90° as shown in Fig. 2(b). Each unit cell features patches of defined width (y) and a spacing (d) between adjacent patches, embedded within 2 µm thick SiO_2 layers. Thus, a 4×4 array aperture of the unit cell was simulated and the characteristics were analyzed. However, this design performs less effectively compared to the DRP-AMC based OCA configuration due to the absence of the gap between parallel rectangular patches, which is a key feature in the DRP-AMC structure illustrated in Fig. 1(b). SRP-AMC characterized only equivalent inductance, L and the capacitance, C, unlike in DRP-AMC with equivalent components consists of C1, C2, Cg capacitance, and L1, L2, and Lg capacitances respectively.

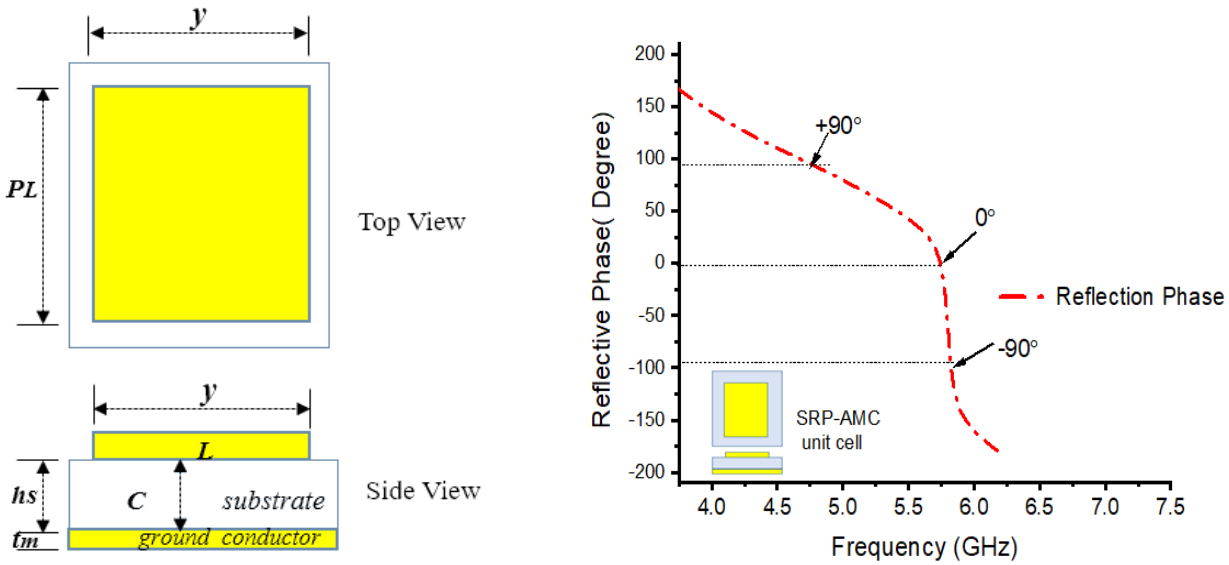

Fig. 2 *A SRP-AMC structure (a) Unit cell geometry; (b) Reflection phase*

2.2 Design of DRP-AMC Structure

A dual rectangular patch (DRP) artificial magnetic conductor (AMC) consists of two parallel reflectors arranged in a 4x4 unit cell configuration. Each cell includes patches with specified width (Pw), the gap between the patch (g), and the substrate height (hs), which was incorporated within SiO2 layers, each of 2 µm thick. This configuration, shown in Fig. 1(a), improves upon single patch unit cells by utilizing the patch gap g to control reflection phase characteristics. The structure induces capacitance (Cg) between patches A and B, with parasitic capacitances (C1, C2) and inductances (L1, L2, Lg) contributing to an equivalent circuit, as shown in Fig. 3(a). Equations (1) and (2) relate these elements to Pw and g, determining resonance frequency and bandwidth (BW) equations (3) and (4). BW varies with inductance, influencing phase shift within -90 to +90 degrees.

$$L = 4\pi\mu_r h_s \times 10^{-7} \tag{1}$$

$$C = 2.82x10^{-12}(1 + \varepsilon)cosh\frac{n(2P_w - g)}{g} \tag{2}$$

$$F = \frac{1}{2\pi\sqrt{LC}} \tag{3}$$

$$BW = \frac{1}{\eta}\sqrt{\frac{L}{C}} \tag{4}$$

Int. Journal of Integrated Engineering Vol. 17 No. 6 (2025) p. 147-158

2.3 DRP-AMC Characteristics

The simulated results from the DRP-AMC model in Fig. 3(a) demonstrate that variations in patch spacing, width, and substrate height significantly influence the characteristics of the AMC, as depicted in Fig. 3(b), where changes in substrate height (hs) impact the reflection coefficient by shift the operational frequency. Equally, variations in the reflection phase affect the model's bandwidth due to changes in capacitance C1 and C2, inversely proportional to the distance to the ground conductor. It was equally observed that change (g) alters capacitance (Cg), influencing the 0-degree reflection phase observed at 5.8 GHz. Configuring the unit cell with boundary conditions can precisely determine this phase at desired frequencies, enhancing antenna performance.

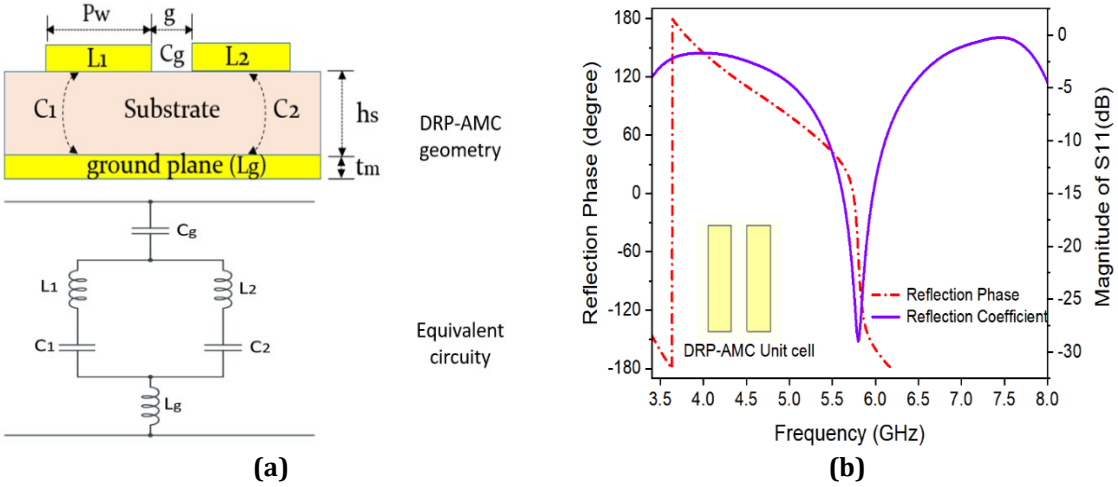

Fig. 3 *A DRP-AMC structure (a) Geometry and equivalent circuit; (b) Reflection phase and coefficient*

2.4 Simulation of the SRP-AMC and DRP-AMC Inspired Antenna Design

In this work, two types of AMC structures were modeled using an SRP and DRP-AMC structures utilizing CST 3D microwave studio environment. Initially, an SRP-AMC unit cell was designed, and its optimal dimensions were obtained with an area of (2.125 × 1.8) mm^2 and a SiO_2 layer thickness of 2 µm. The electromagnetic characteristics of the unit cell were then analyzed. After this, a 4×4 array configuration, as illustrated in Fig. 1(c), was implemented and integrated into the third metal layer (M2) of the chip to serve as a shield against electromagnetic waves emitted by the top antenna radiator. Key antenna parameters such as magnitude of S11, gain, and efficiency were extracted. Fig. 4 shows a comparison of the simulated magnitude of S11(dB), and the antenna gain(dB) for SRP, and the proposed DRP-AMC inspired OCA. Silver (Ag) was selected as the conductor due to its superior electrical conductivity, while silicon dioxide (SiO_2) with a dielectric constant of εr = 3.75 was used as the substrate material. For both SRP-AMC and DRP-AMC designs, a frequency domain solver was utilized to fine-tune the performance by adjusting specific parameters: PL, hs, and y for SRP-AMC, and Pw, hs, and g for DRP-AMC. The DRP-AMC simulation followed the same procedure as that of the SRP-AMC. The optimized AMC parameters are summarized in Table 1. Moreover, comparing the performance of the two AMC models, it was observed that the DRP-AMC design were achieved high performance over the SRP-AMC, with a simulated gain of 3.64 dB, and 2.96 dB respectively. Thus, improved magnitude of S11 over the SRP-AMC inspired design.

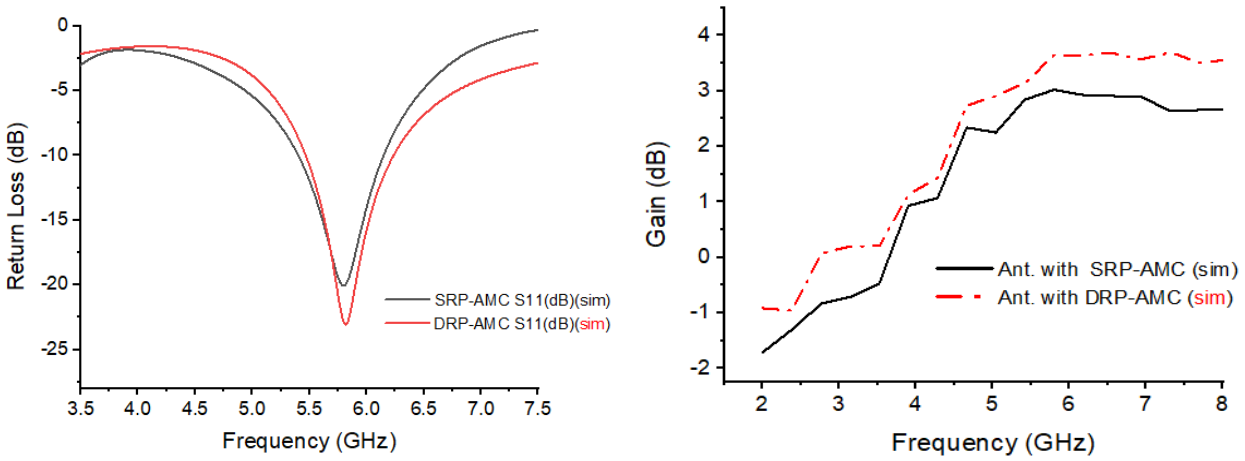

Fig. 4 *Simulated parameters of SRP-AMC inspired OCA (a) Magnitude of (S11); (b) Gain (dB)*

3. Experimental Design and Validation

3.1 Fabrication Process

A proposed work with enhanced gain is fabricated following the process shown in Fig. 5, while the experimental prototype fabrication phases is presented in Fig. 6. The procedural steps are detailed as follows:

Initially, to ensure seamless integration of the multi-layer structures onto the silicon wafer during the sputtering process, a wafer dicing machine was used to precisely cut the 4-inch processed Si-wafer into the required antenna dimensions, as depicted in Step 1

Secondly, a thin-film masks were designed for each metal and SiO_2 layer, including the radiating element, SRP, DRP-AMC structures, and ground plane. To achieve this, a 0.1 mm thin metal film of steel material was used to create the radiator and the DRP-AMC masks, in which a laser machine was then employed to scribe according to the required dimensions in shown in step 2. Then, magnetron sputtering technology was employed for the sputtering process, with silver (Ag) chosen as the target conductor due to its high electrical conductivity and short sputtering duration, as illustrated in Step 3.

To ensure a reliable SMA connection to the sputtered prototype, a ProtoFlow reflow oven was utilized for lead-free reflow soldering. An electrically conductive silver paste (9410-3M) was applied as the mounting paste to secure the surface connection. The reflow process consists of four key stages: pre-heating, soaking, reflow, and cooling. The image in Step 4 showcases the reflow oven technology. Fig. 7(b) is the view of proposed fabricated prototype.

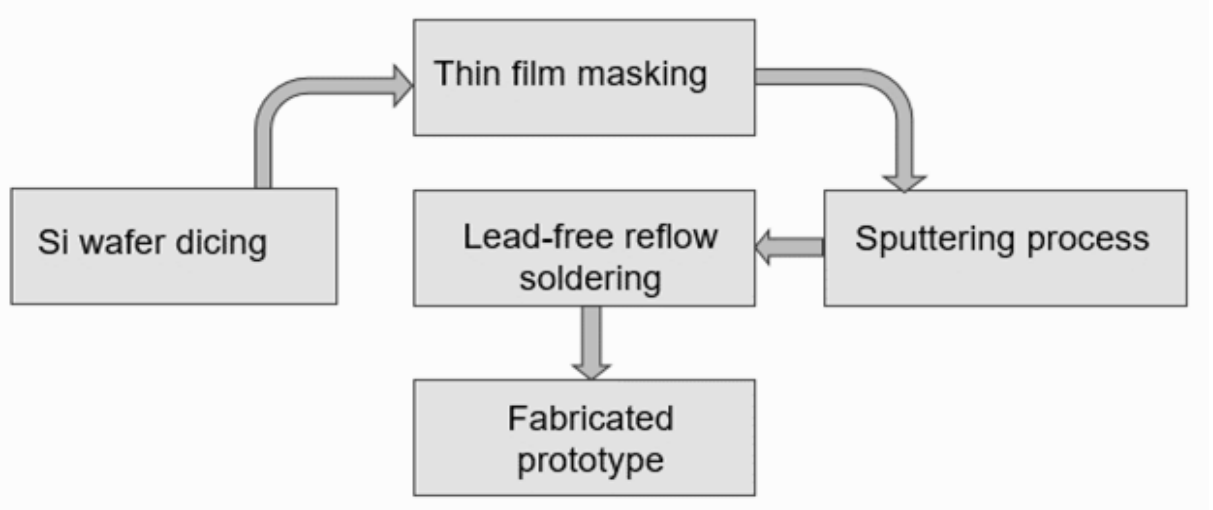

Fig. 5 *The Proposed antenna design (a) 3D simulation model; (b) Fabricated prototype*

Int. Journal of Integrated Engineering Vol. 17 No. 6 (2025) p. 147-158

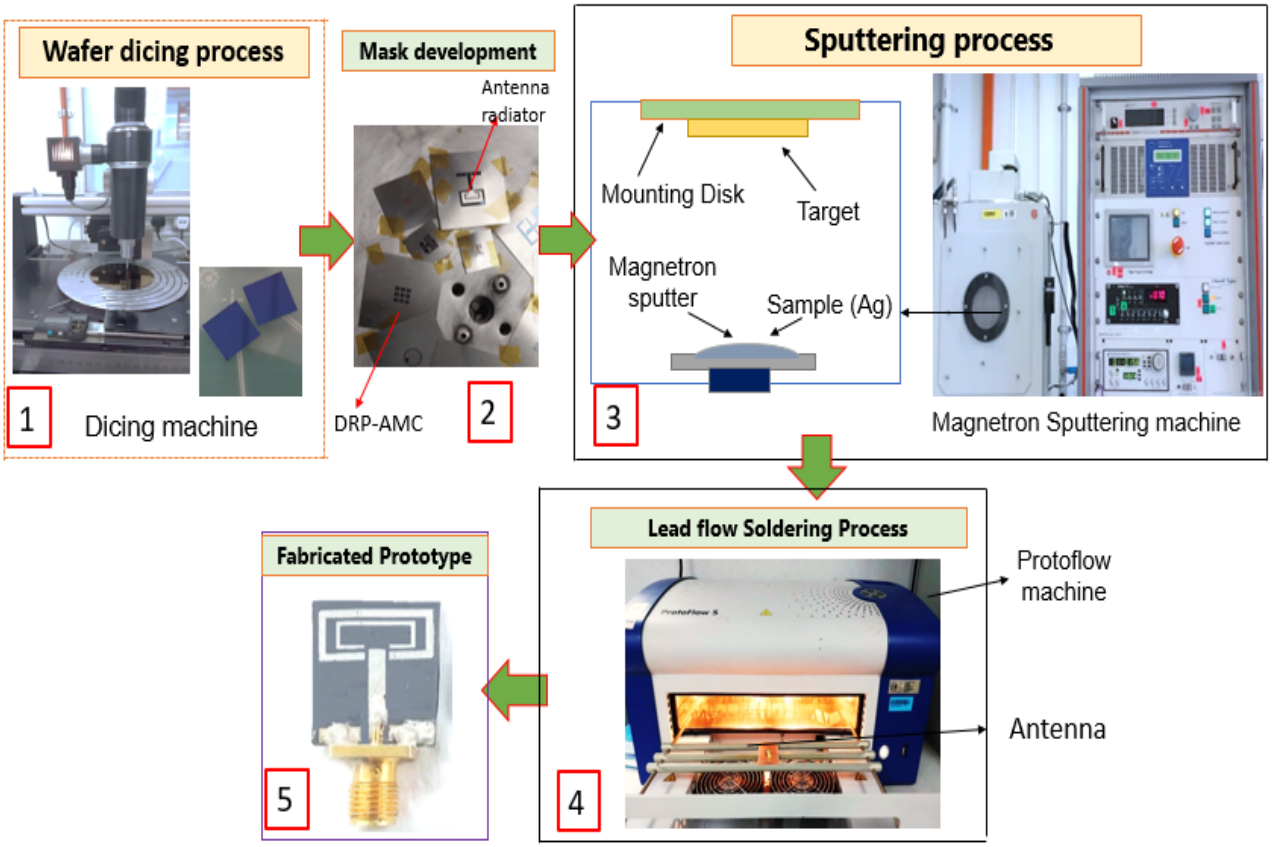

Fig. 6 *Proposed antenna fabrication process*

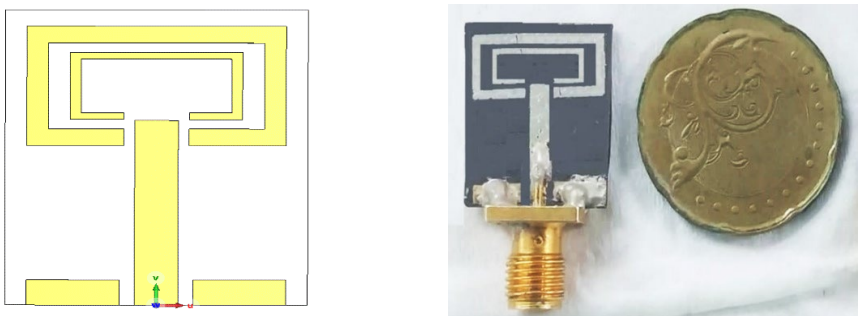

(a) **(b)**

Fig. 7 *The fabricated antenna (a) 3D simulation model; (b) Fabricated prototype*

3.2 Measurement and Validation

It has It is crucial to carry out measurements after each antenna fabrication cycle to validate its performance and ensure consistency with simulation results. Antenna testing is conducted to confirm compliance with standard performance criteria. Key parameters typically measured include return loss, gain, efficiency, impedance bandwidth, and Voltage Standing Wave Ratio (VSWR), among others. In this study, the PNA-X Microwave Network Analyzer (MNA), model N5245A from Keysight Technologies, was employed to measure the S_{11} parameter and determine the impedance bandwidth at resonance. The antenna was designed to operate at a resonance frequency of 5.8 GHz, while the analyzer's frequency sweep was set from 2 GHz to 10 GHz, despite its broader capability of 10 MHz to 50 GHz. The impedance bandwidth was evaluated by identifying the frequency range where return loss remained below -10 dB. Additionally, far-field radiation characteristics were assessed to verify

antenna gain and efficiency. Initial conditions were established using an Agilent 83640B signal generator set to emit 0 dBm at the resonance frequency. Output power was recorded using an N9030A signal analyzer connected to the receiving antenna, with the antenna under test (AUT) positioned at a far-field distance '*r*' from the transmitting antenna (TA). A broadband horn antenna (model LB-20200-SF), featuring a 20 dB gain and operating over the 2–20 GHz frequency range, served as the transmitting antenna. Measurements were conducted at various distances '*r*' to determine the point of maximum gain as expressed in equation (6).

$$r \geq \frac{2D^2}{\lambda} \tag{6}$$

where, r is the far-field distance, D is the maximum linear antenna dimension

In this measurement, the radiation patterns were presented in two-dimensional planes specifically in the E-plane and H-plane, and the experimental setup for radiation pattern and gain measurements within the anechoic chamber is illustrated in Fig. 8.

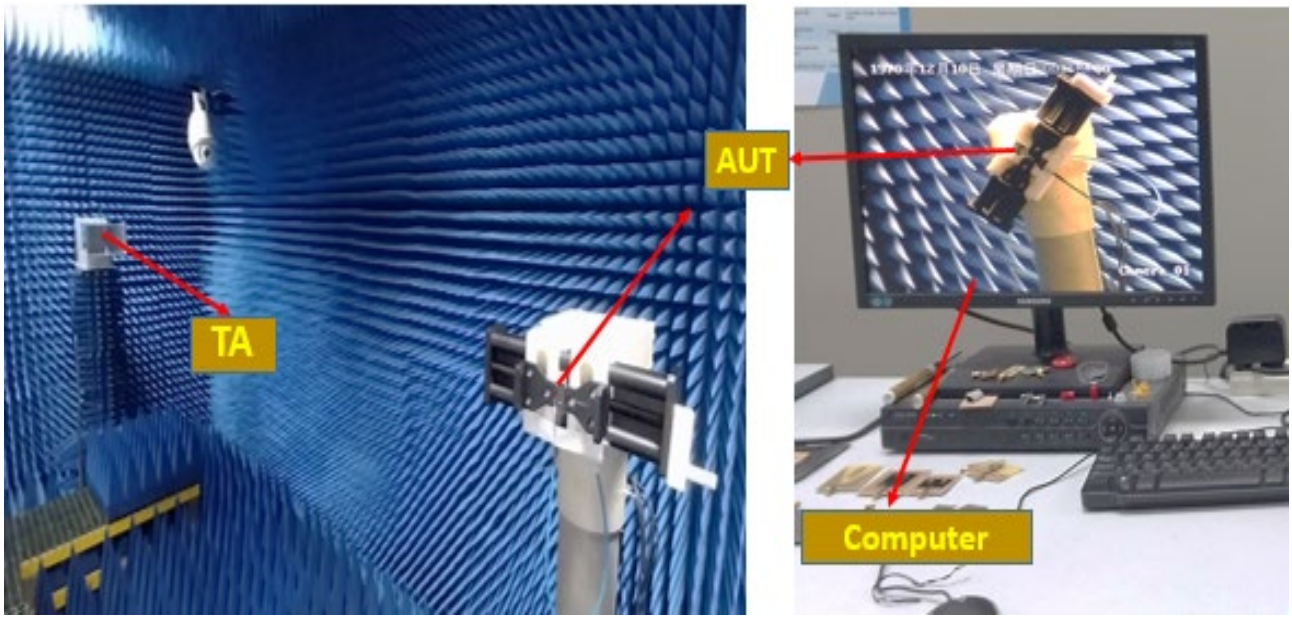

(a) **(b)**

Fig. 8 *The Experimental setup for radiation and gain measurement (a) Anechoic Chamber; (b) Monitoring system*

4. Results and Discussion

In this study, an enhanced-performance OCA operating at 5.8 GHz is introduced. The design incorporates a modified DRP-AMC periodic aperture to enhance the antenna gain, and the radiation characteristics. A monopole planar antenna was integrated as the radiating conductor on the top layer of the chip structure. The model was simulated to determine the characteristics of reflection phase at 0 and ±90 degrees at center frequency. Subsequently, the optimized DRP-AMC model was integrated into the structure. The final design was simulated to determine the antenna parameters including the antenna gain, efficiency, and radiation pattern. A prototype antenna was fabricated, as shown in Fig. 7(b). Thus, measurements were conducted to validate the antenna performance. The measured results show a notable increase in gain, radiation characteristics, and impedance bandwidth compared to the SRP-AMC design. Moreover, Fig. 9(a) compares simulated and measured return loss, whereas Fig. 9(b) depicts the gain outcomes for the antenna with the SRP and DRP-AMC model. It was observed that there are significant differences between the SRP and the DRP-AMC-inspired design results, which can be ascribed to the model's performance compared to the single AMC design. Achieved an improvement of 3.16 dB and radiation efficiency of 62.6 %, a significantly enhanced gain compared to the SRP-AMC with a gain of 2.2 dB, and previous work mentioned in this article. This indicated that the incorporating the DRP-AMC periodic structure within the chip SiO2 layers yield significant changes in both the gain, and radiation characteristic of the antenna over the conventional SRP-AMC design. However, a slight variation exists between the simulated and measured return loss, which might be ascribed to the fabrication tolerances, impedance mismatches, and dielectric losses.

Int. Journal of Integrated Engineering Vol. 17 No. 6 (2025) p. 147-158

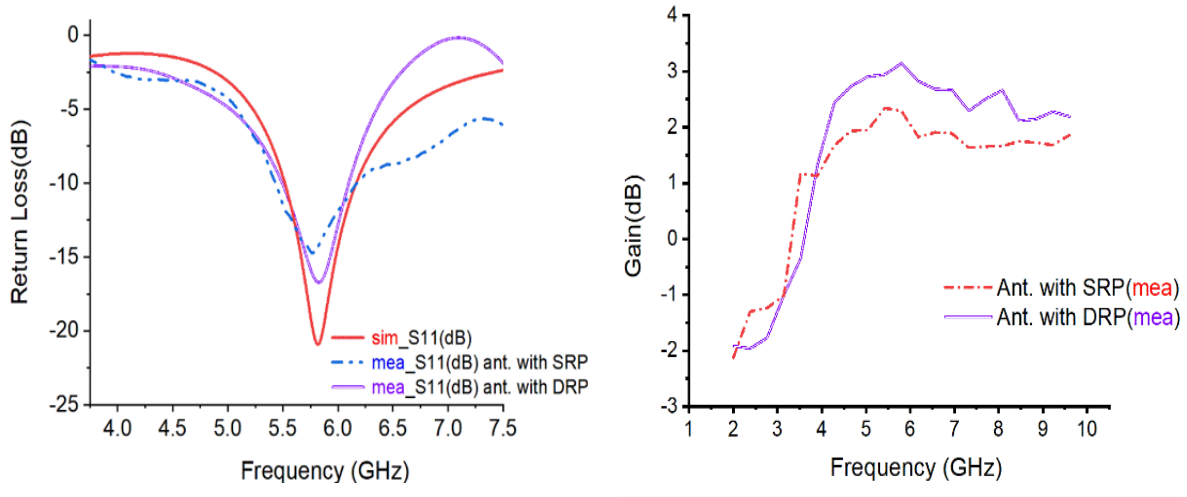

(a) **(b)**

Fig. 9 *Comparison of antenna parameters with SRP and DRP-AMC (a) Simulated and measured (S11); (b) Measured gain (dB)*

4.1 Radiation Pattern

Alongside evaluating the antenna gain and efficiency, the radiation characteristics were equally measured and compared with simulations, then displayed in 2D patterns. Fig. 10 shows the E-plane and H-plane plots, depicting the co- and cross-polarization patterns at 5.8 GHz. The measured and simulated radiation patterns are broadly similar, though minor discrepancies are noted, which are due construction tolerances, impedance mismatches, and dielectric losses.

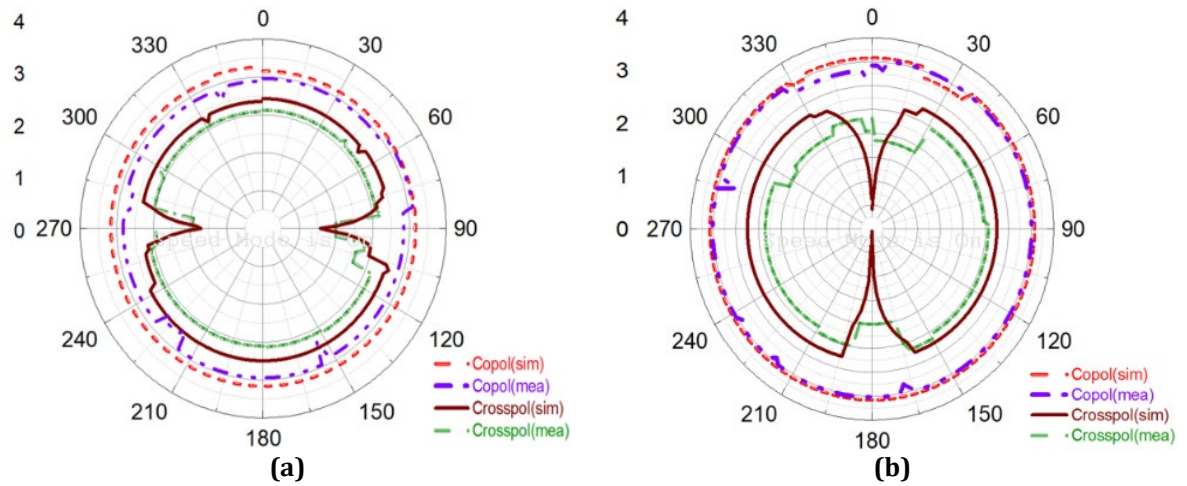

(a) **(b)**

Fig. 10 *The 2D radiation pattern presentation of the antenna (a) E-plane; (b) H-plane at 5.8 GH*

4.2 Effect of DRP-AMC on the Antenna Performance

The reflection phase magnitude affects the properties of the modified AMC, the distance between patches, and the substrate thickness. To evaluate the DRP-AMC's performance, parametric studies were conducted on the variation of the separation gap, g, and its performance. Fig. 11 shows how the AMC impacts the reflection phase, which is crucial for the structure's performance. This effect is due to changes in induced capacitance *Cg* across the patches, as the capacitance is inversely to the distance between the patches. Furthermore, incorporating a 4x4 AMC array into the antenna structure significantly enhanced measured gain to 3.16 dB, achieving improvements of 29.7% over SRP-AMC designs.

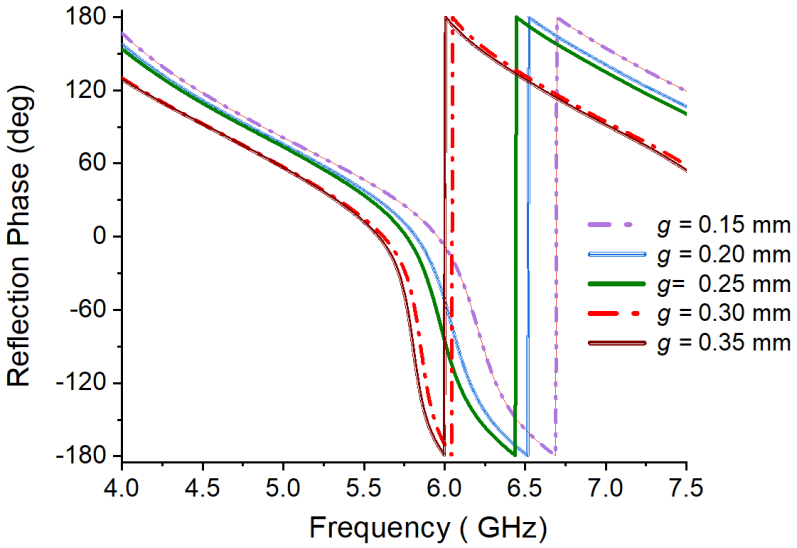

Fig. 11 *Effect of the DRP-AMC on the reflection phase*

4.3 Comparison of Proposed Design with Original and the Previous Works

In this study, two antenna designs were carried out. The first involved the development and fabrication of a multilayer chip antenna incorporating an SRP-AMC as the third layer, as illustrated in Fig. 1(c). This configuration achieved simulated and measured gains of 2.96 dB and 2.2 dB, respectively. To enhance performance, a DRP-AMC design shown in Fig. 1(b) was integrated into the OCA structure, as depicted in Fig. 1(a). This improved version attained peak simulated and measured gains of 3.64 dB and 3.16 dB, respectively. Compared to the initial SRP-AMC-based design, the DRP-AMC variant showed a gain improvement of 0.96 dB and a reflection coefficient (S11) improvement of about -3 dB. These enhancements in gain and reflection characteristics indicate that the DRP-AMC outperformed the SRP-AMC in the OCA design, particularly within the mid-frequency range. Thus, the geometrical difference between the SRP-AMC and DRP-AMC is the two parallel plates for DRP, and single patch for SRP. In which, they differs in total capacitance and inductance due to the separation in DRP. Thus, induction of this gap, significantly enhances the performance of DRP-AMC inspired over the SRP based OCA.

Moreover Table 2, compares significant performance of the proposed design with the contemporary works presented in this work, particularly the gain, and radiation efficiency. It realized that proposed work achieved a working gain of 3.16 dB with radiation efficiency of 62.2% compared to the suggested works in the table, except for folded dipole design presented in [24], and meander dipole OCA presented in [22] with an efficiency of 68.7%, and of 60% respectively. However, a considerable return loss of 48.09 dB was obtained in [[21] over the proposed design in this work. Although, the radiation efficiency realized in [20], and [23] are also considered despite the attainment of the low gain which also attributed to miniature antenna size and inherited properties of silicon substrate. Considering the comparison, it's quite clear that introduction of the DRP-AMC array has led to the significant improvement in both gain and the radiation characteristics of the proposed design.

Table 2 *The comparison of suggested work with previous literature*

Ref	Antenna Type	Freq (GHz)	Size (mm^2)	Peak Gain (dB)	Rad. Eff (%)	Return Loss (dB)
[20]	Monopole meandered	9.45	1.60x1.91	-29.2	21.07	13.2
[21]	Loop	5.8	1.4x1.4	-48.93	NM	48.09
[22]	Meander Dipole	2.4	4.0 x4.0	-23.8 (in Air) -25.9 (in skin)	60	<-10
[23]	Loop	5.8	1.05x0.85	-23.7	NM	
[24]	Folded Dipole	5.8	4.1 x4.0	2.1	68.7	-23
[25]	Folded Loop	2.4	1.5x1.5	-20.8	31.2	NM
This work	Monopole planar	5.8	10.8 x 14.5	3.16	62.2	17.25

5. Conclusion

This study reports an enhanced gain on-chip antenna inspired by DRP structured AMC and its influence on the radiation characteristic at 5.8 GHz. The AMC parameters, the patch gap (g), patch width (Pw), and substrate height (hs), were optimized to achieve the desired AMC characteristic. Thus, optimized DRP-AMC was embedded into the multi-layered OCA structure consists of SiO2, metal films, and Silicon substrate. The design was modeled, and the determined the antenna performance. The peak gain of the antenna was realized at g = 250 µm, Pw = 950 µm and hs = 25 µm. The OCA prototype is constructed and measured to assess the validity of the modeled design. The results show that the proposed DRP-AMC-inspired design realized a maximum gain of 3.16 dB and the radiation efficiency of 62.2%, surpassing both non-AMC and SRP-inspired designs. This improvement indicates that utilizing the DRP-AMC model results in a 40.2% increase in gain over non-AMC design and 29.7% higher than the SRP-incorporated design. It achieved an impedance bandwidth of 0.71 GHz, rendering it well suitable for the application of Wi-Fi 6, WiMAX, and RFID transceivers at 5.8 GHz.

Acknowledgement

We gratefully acknowledge the support provided by the Ministry of Higher Education Malaysia via the Fundamental Research Grant Scheme 218 under FRGS/1/2023/TKO7/USM/01/1

Conflict of Interest

Authors declare that there is no conflict of interests regarding the publication of the paper.

Author Contribution

The authors confirm contribution to the paper as follows: ***study conception and design:*** *Ahmadu Girgiri; Bello Muhammad Abdullahi, Mohd Zamir Pakhuruddin;* ***data collection:*** *Muhammad bello Abdullahi, Mohd Nazri Mahmud, Ahmadu Girgiri;* ***analysis and interpretation of results:*** *Mohd Fadzil Ain, Mohd Nazri Mahmud, Ahmadu Girgiri;* ***draft manuscript preparation:*** *Bello Abdullahi Muhammad, Ahmadu Girgiri. All authors reviewed the results and approved the final version of the manuscript.*

References

[1] Sene, B., Reiter, D., Knapp, H., & Pohl, N. (2022) Design of a cost-efficient monostatic radar sensor with antennaon-chip and lens in package, *IEEE Transactions on Microwave Theory and Techniques*, *70*(1), 502–512, https://doi.org/10.1109/TMTT.2021.3098862

[2] Chen, Z., Liu, Q., Smolders, B., Baltus, P., & Gao, H. (2019) 30-GHz co-designed low-noise amplifier and antenna-on-Chip for Wireless Applications, *2019 IEEE International Symposium on Radio-Frequency Integration Technology, RFIT 2019 - Proceedings*, 5–7, https://doi.org/10.1109/RFIT.2019.8929159

[3] Juneja, S., Pratap, R., & Sharma, R. (2021) Semiconductor technologies for 5G implementation at millimeter wave frequencies – Design challenges and current state of work. *Engineering Science and Technology, an International Journal*, *24*(1), 205–217, https://doi.org/10.1016/j.jestch.2020.06.012

[4] Karim, R., Iftikhar, A., Ijaz, B., & Ben Mabrouk, I. (2019) The potentials, challenges, and future directions of on-chip-antennas for emerging wireless applications—A comprehensive survey, *IEEE Access*, *7*, 173897–173934, https://doi.org/10.1109/ACCESS.2019.2957073

[5] Cheema, H. M, & Shamim, A. (2013) The last barrier: on-chip antennas, *IEEE Microwave Magazine*, *14*(1), 79–91, https://doi.org/10.1109/MMM.2012.2226542

[6] Alibakhshikenari, M., Virdee, B. S., Althuwayb, A. A., Mariyanayagam, D., and Limiti, E. (2021) Compact and low-profile on-chip antenna using underside electromagnetic coupling mechanism for terahertz front-end transceivers. *Electronics*, *10*(11)(2021) ,1264, http://doi:org/10.3390/electronics10111264

[7] Park, J. H., Tran, N. M., Hwang, S. I., Kim, D. I., Choi, K.W. (2021) Design and implementation of 5.8 GHz RF wireless power transfer system, *IEEE Access*, *9*, 168520–168534, https://doi:10.1109/ACCESS.2021.3138221

[8] Cheema, H. M, Fatima Khalid, A. S. (2021) *Antenna-on-chip; Design, Challenges, and Opportunities* (p. 275). ARTECH HOUSE, https://avaxgfx.com/ebooks/113205-antenna-on-chip-design-challenges-

[9] Kushwaha, R. K., Karuppanan, P., & Dewang, R. K. (2020) Design of a SIW on-chip antenna using 0.18-µm CMOS process technology at 0.4 THz, *Optik*, *223*(June), 165509, https://doi.org/10.1016/j.ijleo.2020.165509

[10] Althuwayb, A.A., Alibakhshikenari, M., Virdee, B. S., Benetatos, H., Falcone, F., and Limiti, E. (2021) Antenna on chip (AoC) design using metasurface and siw technologies for thz wireless applications. *Electron*., *10*(9), 1-8, https://doi.org/10.3390/electronics10091120

[11] Nafe, M., Syed, A., & Shamim, A. (2017) Gain-enhanced on-chip folded dipole antenna utilizing artificial magnetic conductor at 94 GHz, *IEEE Antennas and Wireless Propagation Letters*, *16*(c), 2844–2847, https://doi.org/10.1109/LAWP.2017.2749308

[12] Ng, H. J., Wang, R., & Kissinger, D. (2019) On-chip antennas in SiGe BiCMOS technology: Challenges, state of the art and future directions, *Asia-Pacific Microwave Conference Proceedings, APMC*, *2018-Novem*, 621–623, https://doi.org/10.23919/APMC.2018.8617626

[13] Yu, Y., Akhter, Z., & Shamim, A. (2023) Improving the performance of antenna-on-chip by effectively illuminating the artificial magnetic conductors through coupling enhancement structures, *IEEE Transactions on Antennas and Propagation*, *71*(5), 4492–4497, https://doi.org/10.1109/TAP.2023.3239102

[14] Atif Shamim, & Haoran Zhang. (2020). On-chip antenna: challenges and design considerations. In Q. H. Abbasi, S. F. Jilani, A. Alomainy, & M. A. Imran (Eds.), *Antennas and Propagation for 5G and Beyond* (pp. 123–155). Institution of Engineering and Technology, https://doi.org/10.1049/PBTE093E_ch6

[15] Othman, N., Samsuri, N. A., Rahim, M. K. A., & Kamardin, K. (2020) Low specific absorption rate and gain-enhanced meandered bowtie antenna utilizing flexible dipole-like artificial magnetic conductor for medical application at 2.4 GHz, *Microwave and Optical Technology Letters*, *62*(12), 3881–3889, https://doi.org/10.1002/mop.32507

[16] Mohammad, A., Virde, B. S., Salekzamankhnani, S., Babaeian, F., Ali, S.M., Iqbal, A., and Al-Hasan, M. (2023) On-chip terahertz antenna array bsed on amalgamation of metasurface-inspired and artificial magnetic conductor technologies for next generation of wireless slectronic devices, *AEU-International Journal of Electronics and Communication*, *167,* 154684, https://doi.org/10.1016/j.aeue.2023.154684

[17] Liu, Q., Van Den Biggelaar, A. J., Johannsen, U., Van Beurden, M. C., Smolders, A. B., & Cheema, H. M. (2020) On-chip metal tiling for improving grounded mm-wave antenna-on-chip performance in standard low-cost packaging, *IEEE Transactions on Antennas and Propagation*, *68*(4), 2638–2645, https://doi.org/10.1109/TAP.2019.2957713.

[18] Knyazev, M. A., Soltanovich, O.A., Sedlovets, D. M., & Korotitsky, V.I. (2023) Electrical properties of silicon oxide layers subjected to high - temperature treatment reproducing the growth conditions for thin carbon films, Journal of Electronic Materials, 52(8), 5159–5165, https://doi:10.1007/s11664-023-10498-4.

[19] Karim, R., Iftikhar, A., & Ramzan, R. (2020) Performance-Issues-Mitigation-Techniques for on-chip-antennas – Recent developments in RF, mm-wave, and THz bands with future directions, *IEEE Access*, *8*, 219577–219610, https://doi.org/10.1109/ACCESS.2020.3042928

[20] Singh, H., & Mandal, S. K. (2020). Miniaturized on-chip meandered loop antenna with improved gain using partially shield layer, In *European Conference on Antennas and Propagation, EuCAP 2020*, 13–16, https://doi.org/10.23919/EuCAP48036.2020.9136025

[21] Razak, A. H. A., Shamsuddin, M. I. A., Idros, M. F. M., Halim, A. K., Ahmad, A., & Junid, S. A. M. A. (2018). Design of 5.8 GHz integrated antenna on 180nm complementary metal oxide semiconductor (CMOS) technology. *IOP Conference Series: Materials Science and Engineering*, *341*(1), https://doi.org/10.1088/1757-899X/341/1/012015

[22] Ray, A., De, A., & Bhattacharyya, T. K. (2021). A package-cognizant CMOS on-chip antenna for 2.4 GHz free-space and implantable applications, *IEEE Transactions on Antennas and Propagation*, *69*(11), 7355–7363, https://doi.org/10.1109/TAP.2021.3076555

[23] Charlot, E., Hamada, M., & Kuroda, T. (2021) An on-chip antenna with an area of 0.9 square millimeters for RFID applications in the 5.8 GHz - 24 GHz range, In *International Symposium on Antennas and Propagation, ISAP 2020*, 41–42, https://doi.org/10.23919/ISAP47053.2021.9391369

[24] Girgiri, A., Ain, M. F., Muhammad, B. A., & Mohammed, A. S (2023) Design of miniaturized folded dipole integrated on-chip antenna for 5.8GHz application, In *IEEE International Symposium on Antennas and Propagation, ISAP*, https://doi.org/10.1109/ISAP57493.2023.10389045

[25] Archana, S & Bhaskar, M. (2023) An Integrated 2.4 GHz Inductorless power amplifier and on-chip two turn folded loop antenna for biotelemetry applications. *14th International Conference on Computing Communication and Networking Technologies(ICCCNT)*, Delhi, India, pp. 1-6,https;//doi: 10.1109/ICCCNT56998.2023.10307385